Supplementary Information (ESI) for

Nanocomposite of nickel oxide nanoparticles and polyethylene oxide as printable hole injection layer for organic solar cells

Marta Ruscello[a], Tanmoy Sarkar[b], Artem Levitsky[b], Giovanni Maria Matrone[c], Nikolaos Droseros[d], Stefan Schlisske[a,e], Eleni Sachs[a,e], Patrick Reiser[a,f], Eric Mankel[a,f], Wolfgang Kowalsky[a,g], Natalie Banerji[d], Natalie Stingelin[c,h], Gitti L. Frey[b], and Gerardo Hernandez-Sosa*[a,e]

a. InnovationLab GmbH, Speyerer Strasse 4, 69115 Heidelberg, Germany

b. Department of Materials Science and Engineering, Technion – Israel Institute of Technology, Haifa 32000, Israel.

c. Department of Materials and Centre for Plastic Electronics, Imperial College London, London SW7 2AZ, UK

d. Department of Chemistry and Biochemistry, University of Bern, Freiestrasse 3, CH-3012 Bern, Switzerland

e. Light Technology Institute, Karlsruhe Institute of Technology, Engesserstrasse 13, 76131 Karlsruhe, Germany. E-mail: gerardo.sosa@kit.edu

f. Surface Science Division, Materials Science Department, Technische Universität Darmstadt, Jovanka-Bontschits-Straße 2, 64287 Darmstadt, Germany

g. Institut für Hochfrequenztechnik, Technische Universität Braunschweig, Schleinitzstrasse 22, 38106 Braunschweig, Germany

h. School of Materials Science & Engineering and School of Chemical & Biomolecular Engineering, Georgia Institute of Technology, Ferst Drive, Atlanta, Georgia 30332, United States

	Before Plasma		After Plasma	
	Thickness (nm)	Refractive index (n)	Thickness (nm)	Refractive index (n)
NiO_x	14.3	1.72	13.6	1.73
NiO_x:PEO 70% wt	13	1.78	7.9	1.88
NiO_x:PEO 40% wt	8.3	1.8	3.2	1.8
NiO_x:PEO 30% wt	8.7	1.9	3.4	1.85
PEO	1	1.24	0.5	1.24

Table S1. Thicknesses of layers with different NiO_x content determined by ellipsometry, before and after oxygen plasma treatment.

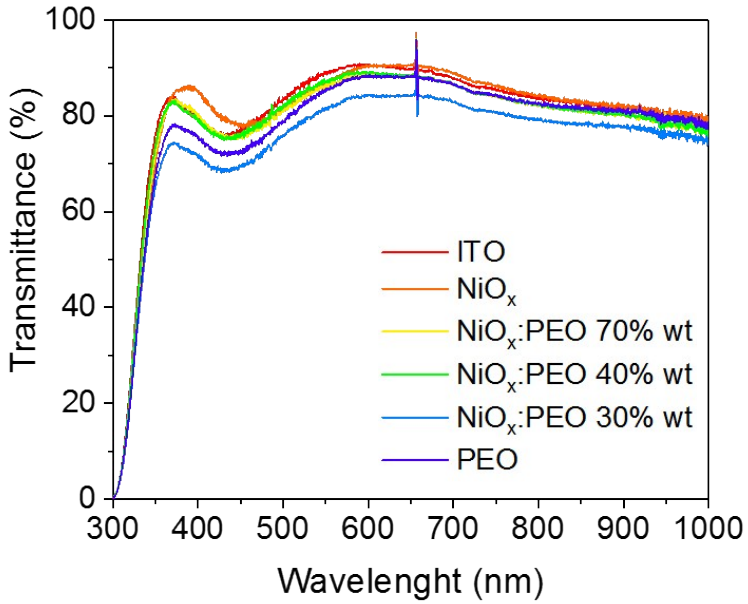

Figure S1. Transmission spectra of layers with different NiO_x content

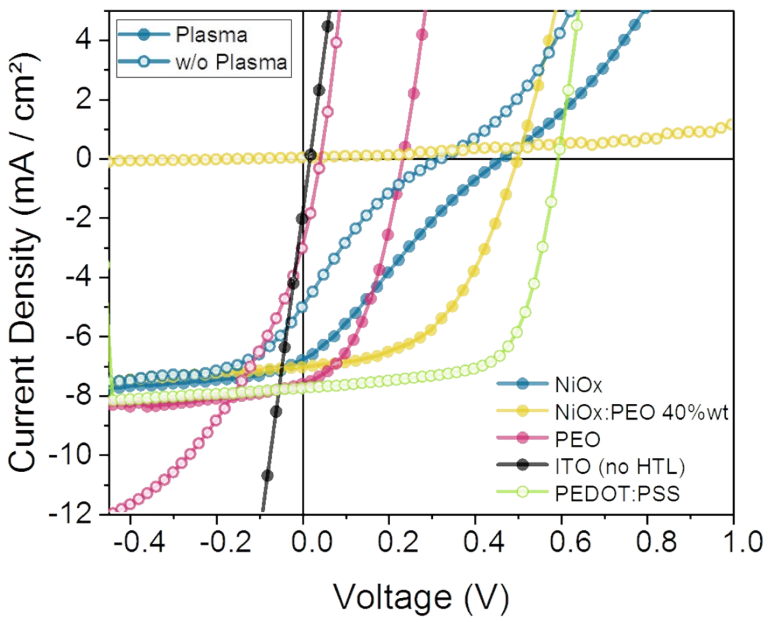

Figure S2. I-V curves of selected solar cells (spin coated) with bare ITO, PEDOT:PSS or different NiO_x concentration, with or without oxygen plasma treatment before the active layer deposition.

Concerning the no HTL samples, it is worth noting that the yield for such devices is very low due to high incidence of roughness induced shortcuts. Compared with PEDOT:PSS, there is a difference in all of the cell parameters, resulting in an efficiency for PEDOT:PSS PCE = 3.00% and confirming the quality of the active layer used.

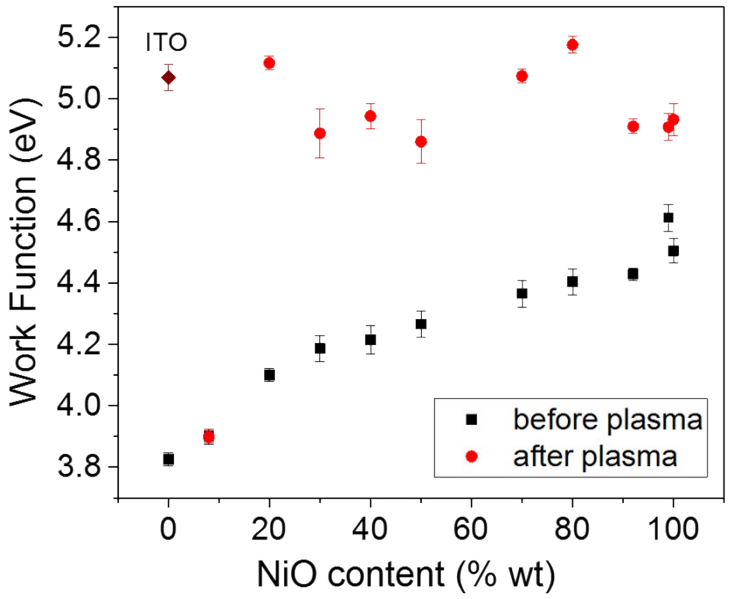

Fig. S3: Work-function of PEO, NiOx:PEO and NiOx layers, before and after plasma treatment, measured by Kelvin Probe.

It has already been shown in literature that the treatment of the deposited film with oxygen plasma for short times has remarkable effect on the electrical properties of the NiO_x nanoparticles, as it can be ascribed to a further oxidation of the NiO species operated by the plasma which allows the formation of the more conductive species NiOOH and causes a jump in the WF up to >0.5 eV.[24,38,39] It can be noted for the pure NiO_x nanoparticles that the shift in the WF caused by the plasma treatment is less extensive than literature, with a ΔWF = 0.43 eV (increases from 4.50 to 4.93 eV); while it is more evident in the case of the blends, as for the NiO_x:PEO 40:60%wt where the shift is ΔWF = 0.73 eV. Increasing content of PEO brings the WF from 4.50 eV for the pristine NiO_x film to values close to 3.83 eV of the PEO alone. Through oxygen plasma treatment, the optimal WF (around 5.0 eV or higher) is reached independently from the PEO content for the same plasma treatment.

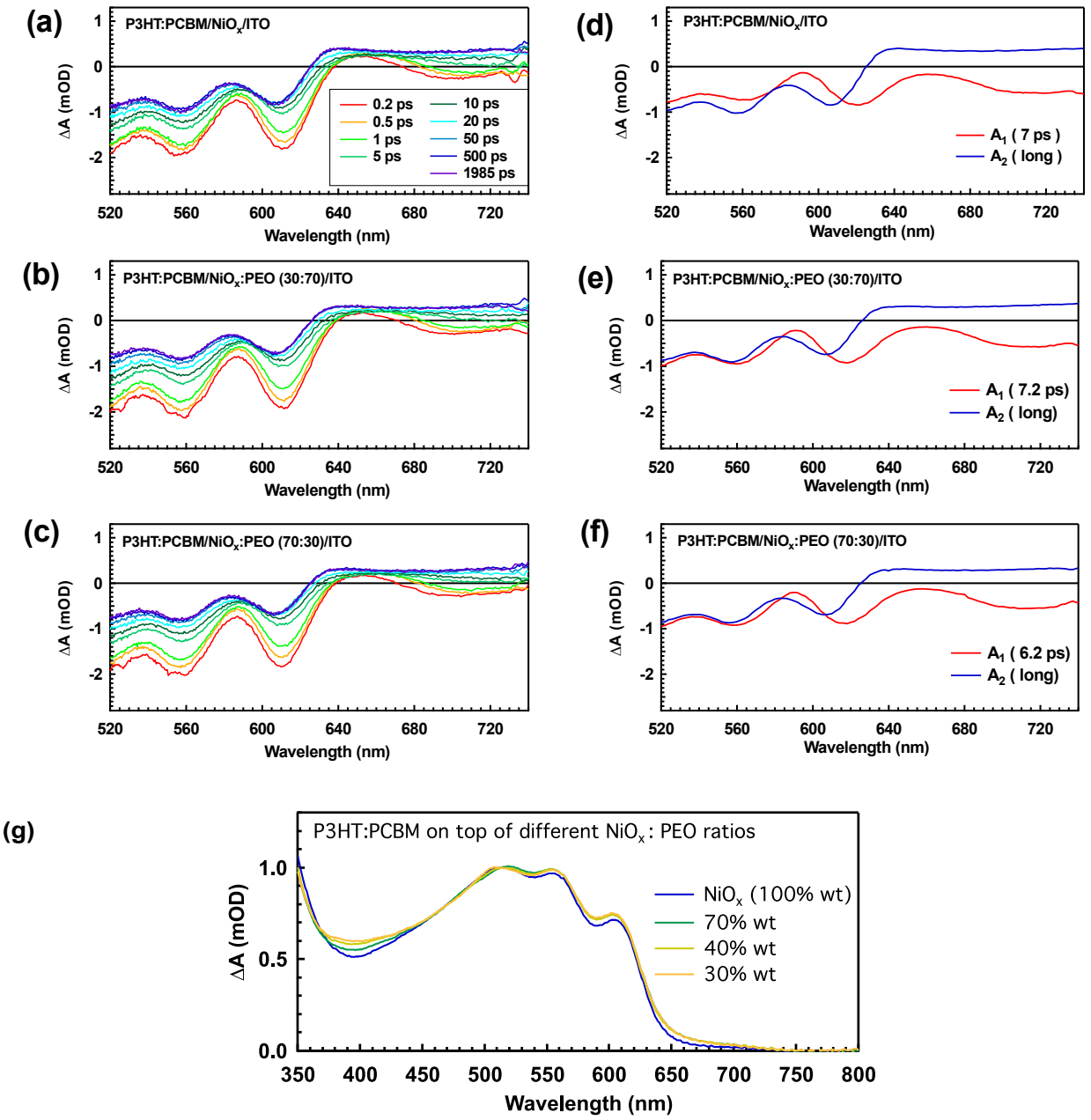

Fig. S4: (a - c) TA Spectra recorded at different time delays after excitation with 500 nm pulses and (d - f) DAS of the P3HT:PCBM (1:0.9) blends deposited on substrates containing different NiO_x : PEO ratios. (g) Steady state absorption spectra of P3HT:PCBM blends deposited on top of substrates containing different NiO_x:PEO ratios. The spectra are normalized at the 515 nm peak.

All measurements were performed with 500 nm pulsed excitation generated by frequency-converting the fundamental beam of an amplified Ti:sapphire laser system (35 fs, 800 nm, 1 kHz, 6 mJ, Astrella Coherent) in an optical parametric amplifier (OPA, Opera Solo, Coherent). Subsequently they were chopped at half the laser frequency. The broadband white light probe pulses were generated by focusing the fundamental beam on a sapphire plate, then split into a reference and a signal component. The signal probe pulses transmitted through

the sample and the reference probe pulses were spectrally dispersed in two home-build prism spectrographs, one for the visible and one for the n-IR, assembled by Entwicklungsbüro Stresing, Berlin and detected separately, shot-to-shot, by a pair of charge-coupled devices (CCD detectors, Hamamatsu S07030-0906). The probe pulses were temporally delayed relative to the excitation pulses via a micrometer translation stage, and pump-probe delays up to 2 ns were measured. The relative polarization of the probe and pump pulses was set to the magic angle, in order for polarization effects to be excluded. The pump and probe beams diameters were measured with a beam profilometer to be 1 mm and 280 μm, respectively, ensuring a uniform distribution of detected photo-excited species. Details on the global analysis procedure can be found in ref. 4 of the SI.[4]

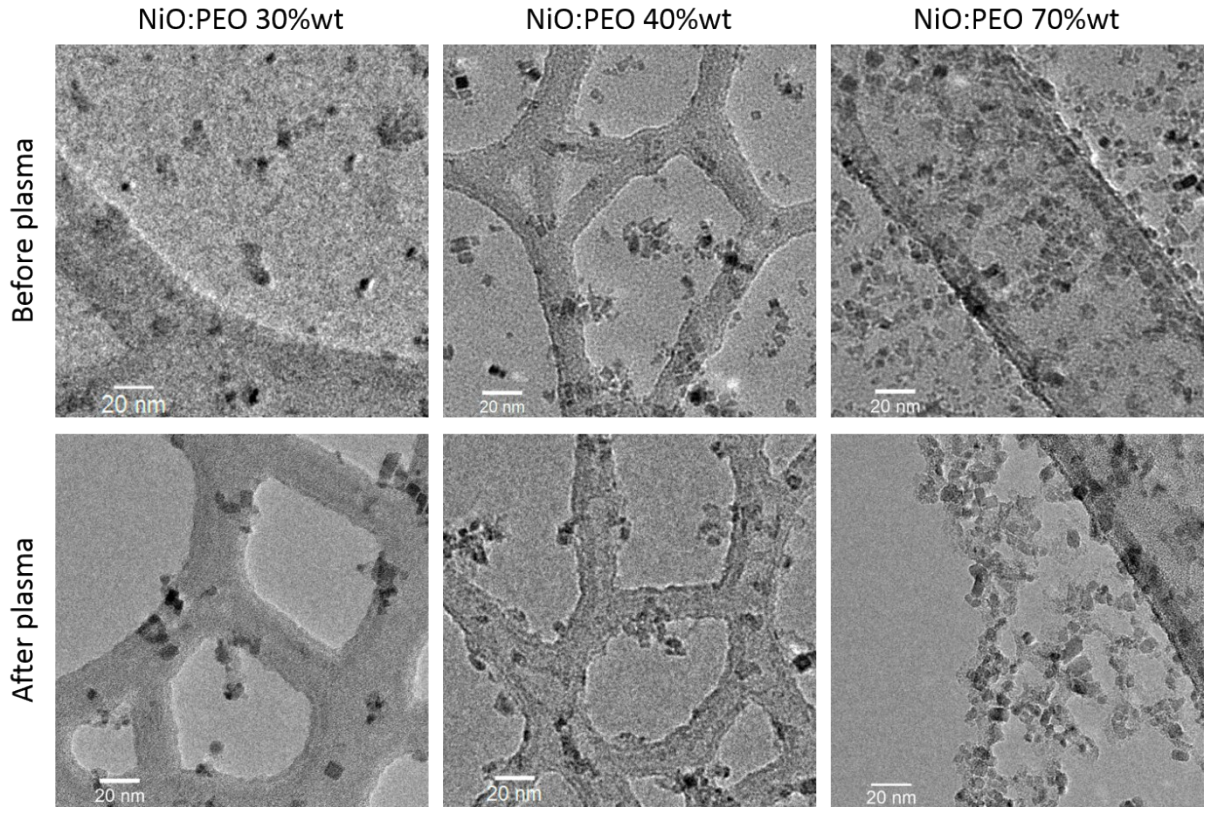

Figure S5. TEM images of NiO_x:PEO blends with different NiO_x content in proximity of the carbon grid before and after oxygen plasma treatment.

Before the plasma treatment, the NiOx particles are dispersed on the grid itself and on the PEO matrix formed between the grid lines. After the plasma treatment, NiOx particles are observed only on the grid itself. These results confirms that the plasma treatment removes the PEO leaving behind only NiOx particles

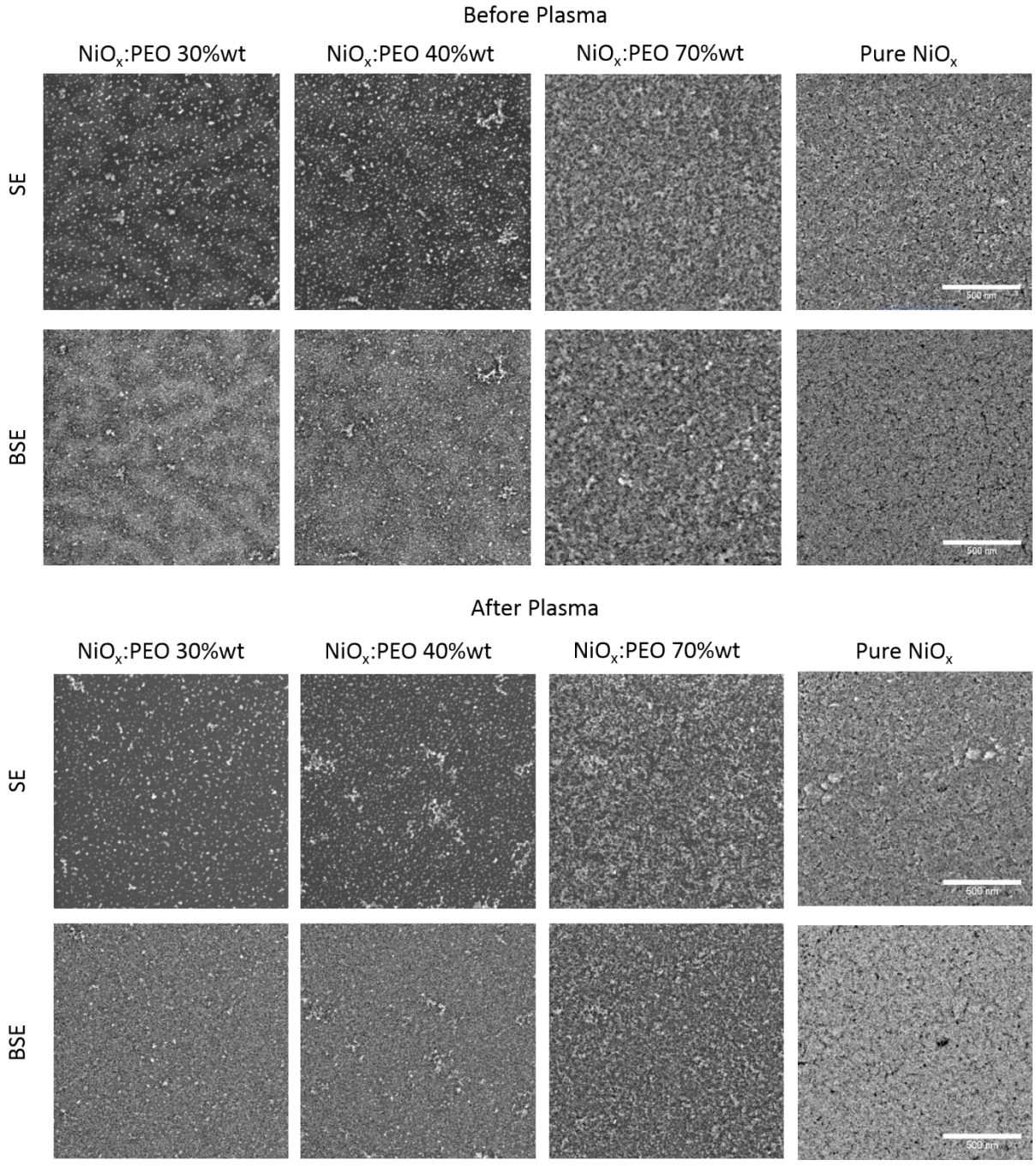

Figure S6. SEM images of NiO_x:PEO blends with different NiO_x content and pure NiO_x before and after oxygen plasma treatment. Scale bar is 500 nm.

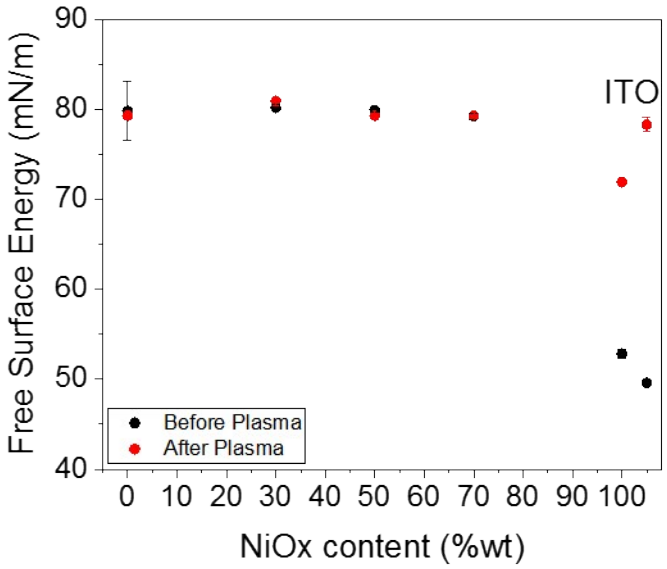

Figure S7. Free surface energy of layers with different NiO_x content, before and after oxygen plasma treatment

Table S2. Contact Angle measurements for water and diiodomethane, of layers with different NiO_x content, before and after oxygen plasma treatment.

	Contact Angle Before Plasma		**Contact Angle After Plasma**	
	Water	**Diiodomethane**	**Water**	**Diiodomethane**
ITO	61.45 (±0.71)	35.09 (±0.37)	9.39 (±0.54)	26.02 (±1.53)
NiO_x	61.45 (±0.71)	35.09 (±0.37)	32.61 (±0.32)	17.40 (±0.19)
NiO_x:PEO 70% wt	12.88 (±0.70)	14.78 (±0.82)	7.43 (±0.36)	21.65 (±0.12)
NiO_x:PEO 40% wt	10.31 (±0.40)	12.79 (±0.60)	7.43 (±0.36)	21.65 (±0.12)
NiO_x:PEO 30% wt	8.41 (±0.17)	13.43 (±1.12)	6.67 (±0.17)	6.19 (±0.85)
PEO	11.25 (±0.67)	11.80 (±12.22)	7.43 (±0.36)	21.65 (±0.12)

The wettability of ITO and NiO_x before and after oxygen plasma treatment are comparable. The total SFE changes for ITO and NiO_x from 52.85 mN/m to 71.9 and 78.3 mN/m, respectively. Especially the contact angle of H_2O undergoes a significant change from 61.45° before plasma to 9.39° and 32.61° after plasma on ITO and NiO_x respectively. The contact angles of both, H_2O and DIM on PEO before the plasma treatment are very small (11.25° and 11.8°) which is related to the high SFE of pristine PEO. Thus, the subsequent plasma treatment does not alter the SFE significantly. Considering the etching effect of the oxygen plasma treatment, the SFE of the plasma treated ITO and PEO cannot be distinguished from each other. The predominant high

SFE of PEO is also present in the blends. Both, the contact angles of water and NiO_x are comparable to them of pure PEO, making the blends highly wettable even before the oxygen plasma treatment. The high SFE of the neat films and the blends after plasma is related to a good wettability for the subsequent solution processed active layer. We therefore conclude that the solution processing of P3HT:PCBM on top of the plasma treated NiO_x as well as on the NiO_x:PEO blends is facilitated and should be favored by the high SFE of the underlying films.

Bibliography

1. B. Mustafa, J. Griffin, A. S. Alsulami, D. G. Lidzey and A. R. Buckley, *Appl. Phys. Lett.*, **2014**, 104, 6–11.
2. H. Zhang, J. Cheng, F. Lin, H. He, J. Mao, K. S. Wong, A. K. Y. Jen and W. C. H. Choy, *ACS Nano*, **2016**, 10, 1503–1511.
3. K.-C. Wang, J.-Y. Jeng, P.-S. Shen, Y.-C. Chang, E. W.-G. Diau, C.-H. Tsai, T.-Y. Chao, H.-C. Hsu, P.-Y. Lin, P. Chen, T.-F. Guo and T.-C. Wen, *Sci. Rep.*, **2014**, 4, 4756.
4. Brauer, J. C.; Lee, Y. H.; Nazeeruddin, M. K.; Banerji, N. *J. Phys. Chem. Lett.* **2015**, 3675–3681.